Molecular BioSystems

Accepted Manuscript

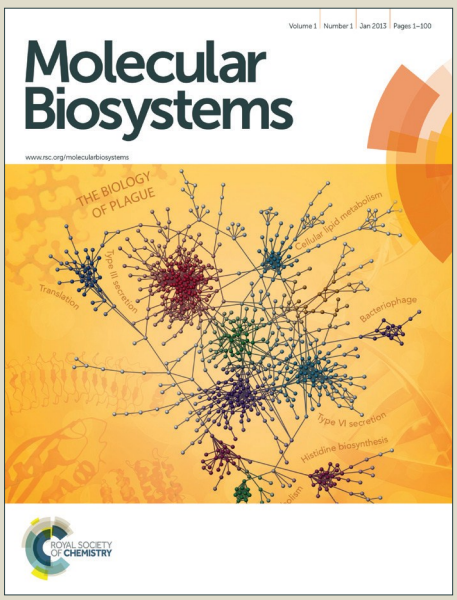

ROYAL SOCIETY OF CHEMISTRY

www.rsc.org/molecularbiosystems

Flap Dynamics of Plasmepsin Proteases: Proposed Parameters and Molecular Dynamics Insight

Wilson Karubiu[a], Soumendranath Bhakat[a], Lara McGillewie[a] and Mahmoud E.S. Soliman[a*]

[a]School of Health Sciences, University of KwaZulu-Natal, Westville, Durban-4000, South Africa

*Corresponding author: Mahmoud E. S. Soliman (email: soliman@ukzn.ac.za)

Graphical Abstract

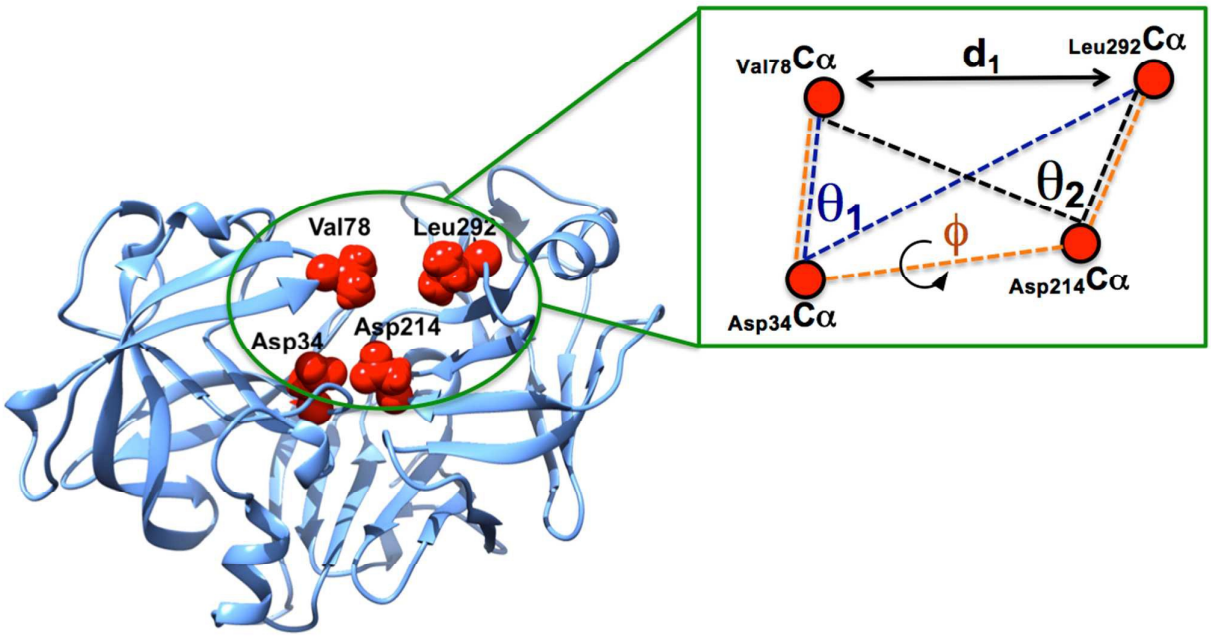

Abstract

Herein, for the first time, we report the flap opening and closing in Plasmepsin proteases – plasmepsin II (PlmII) was used as a prototype model. We proposed different combined parameters to define the asymmetric flap motion; distance, d_1, between the flaps tips residues (Val78 and Leu292); dihedral angle, ϕ; in addition to TriCα angles Val78-Asp34-Leu292, θ_1, and Val78-Asp214-Leu292, θ_2. Only three combined parameters, distance, d_1, dihedral angle, ϕ and TriCα angle, θ_1 were found to appropriately define the observed "twisting' motion during the flap opening and closing. The coordinated motions of the proline-rich loop adjacent to the binding cavity rim appeared to exert steric hindrance on the flap residues, driving the flap away from the active site cavity. This loop may also have increased movements around the catalytic dyad residue, Asp214, making the TriCα, θ_2 unreliable in describing the flap motion. The full flap opening at d_1, 23.6Å corresponded to the largest TriCα angle, θ_1 at 78.6° at ~46 ns time scale. Overall the average θ_1 and θ_2 for the bound was ~46° and ~53°, respectively compared to ~50° and ~59° for the Apo PlmII, indicating a drastic increase in the TriCα as the active site cavity opens. Similar trends in the distance, d_1 and dihedral angle, ϕ were observed during the simulation. The asymmetrical opening of the binding cavity was best described by the large shift in ϕ from -33.91° to +21.00° corresponding to the partial opening of the flap at a range of 22-31ns. Though, the dihedral angle described the twisting of the flap, the extent of flap opening can appropriately be defined by combining the d_1 and the θ_1. The results presented here, on the combined parameters, will certainly augment current efforts in designing potent structure-based inhibitors against plasmepsins.

1. Introduction

The plethora of proteomics data on human pathogens has significantly augmented disease fighting strategies. *Plasmodium falciparum* is responsible for the most lethal form of malaria among the six known *Plasmodium spp*.(*1-3*). Plasmepsins (Plm) are plasmodium encoded proteins, similar to human pepsins, which play critical roles in the erythrocytic stages of plasmodium life cycle (*4*). Currently, only crystal structures of food vacuole plasmepsins (I, II, III, and IV) are available (*5-8*). Plasmepsin II (PlmII), an aspartic protease encoded by *P. falciparum*, has been reported as a virulence factor in malaria where it is involved in haemoglobin degradation. Similar to other aspartic proteases, the PlmII active site contains two aspartic acid residues, a proton donor and acceptor, forming the catalytic dyad when cleaving the peptide bond. General features from experimental studies by Asojo *et al,* show a mature enzyme crystal structure consisting of a single chain, composed of 329 amino acid residues which fold into two topologically similar N and C terminal domains (*6*). The domains make contact along the bottom of the binding cleft, that contains the catalytic dyad Asp34 and Asp214. A single long β hairpin structure (flap, Lys72-Phe85) lies perpendicularly over the binding cleft and lying opposite is a flexible flap-like loop structure (*6, 9*). These two structures are highly flexible where they interact with bound inhibitors and presumably substrates. The amino and carboxyl ends of the polypeptide chain of PlmII are assembled into a characteristic six-stranded interdomain β-sheet which serves to anchor the domains together (*6, 9*).

Several non-structural proteins display unique and specific motions which are essential in defining their precise function(*10*). Determining the correct parameters which best describe such motions in proteins, is essential in understanding enzyme functions as well as its impact on drug binding and resistance. For instance, flap dynamics is a distinctive motion observed amongst aspartate proteases e.g. HIV protease and cathespin. Flaps have been shown to regulate access to the active site of proteases by providing access for substrate and/or inhibitors binding (*10, 11*). Flap opening and closure in HIV protease have been well studied using molecular dynamics (*11-19*). Generally, different parameters have been proposed to describe the HIV PR flap motion (*16*). The distance between Ile50-Ile50' (interflap distance) is one of the most commonly used parameter for defining flap motions. However, this parameter does not adequately describe the curling behaviour observed, which lead to the introduction of other parameters such as curling to better define HIV protease flap dynamics (*19, 20*). The flap dynamics in HIV protease is one such example, which highlights the

importance of defining the appropriate parameters that best describe specific dynamics associated with inhibitor binding to the binding cavity.

The characteristic flap and flap-like structure have been reported to be highly flexible in plasmepsins I-IV, in both the free and ligand-bound proteases relative to other enzyme structures (*5-8*). These structures are critical determinants in the conformational flexibility of the binding cavity of PlmII in accommodating different inhibitors, where crystallographic studies have demonstrated structural differences between the free and ligand-bound enzymes (*6, 9*). Precise insight into the mechanistic events associated with binding of plasmepsins inhibitors is essential for the design of more potent inhibitors. Crystallographic studies reveal that the binding cavity of PlmII is a highly flexible pocket, thus designing more potent inhibitors will require a better understanding of the plasticity of this cavity in response to different inhibitors. Moreover, different inhibitors have shown a varying scale of binding potential to the binding cavity of PlmII. Experimental parameters previously defined are insufficient in examining and predicting the binding modes and flap dynamics of different inhibitors (*6, 9, 21*). The interaction of the PlmII flap pocket with non-peptidomimetic inhibitors have been documented elsewhere (*22*). Therefore, defining appropriate parameters to assess flap motions is critical. Furthermore, the exact parameters to precisely describe flap opening and closing are not well defined in literature, neither experimentally nor computationally. This has prompted us to report the first detailed computational study that highlights the flap dynamics amongst plasmepsins and different proposed parameters. We believe that this article will serve as a benchmark for observing this phenomenon in plasmepsins, potentially other proteases.

2. Methods

2.1.System preparation

The apo crystal structure (PDB ID: 1LF4)(*6*) and complex structure of plasmepsin II (PlmII) bound with potent inhibitor EH58 (PDB ID: 1LF3) (*6*) were obtained from the RSCB Protein Data Bank (*23*). The systems were prepared as described in our previous reports (*24, 25*).

2.2. Molecular dynamic analysis

An all atom explicit solvation molecular dynamics simulation was performed using GPU version of PMEMD engine integrated with Amber14 (*26*). All the systems were set up using the standard methodology discussed in our previous reports (*24, 27*). Visualisation of enzyme

structures was carried out using graphical user interface of UCSF Chimera package(*28*) and data were plotted using the GUI of Microcal Origin data analysis software version 6 (www.originlab.com) and Surfer version 12 (www.goldensoftware.com).

3. Results and Discussion

3.1.Experimentally Determined Parameter and Its Limitations

X-ray diffraction studies on PlmII found that the uncomplexed form (PDB ID: 1LF4) (*6*) of the enzyme is more open than the bound, by measuring the distance between Cα of Val78 at the flap tip and Cα Leu292 on the opposite side of the hydrophobic rim of the binding cavity. In the free enzyme crystal structure, this distance was found to be 12.6Å. However, upon binding to EH58 inhibitor (PDB ID: 1LF3) (*6*) this distance slightly reduced to 12.0Å, indicating the closing of the flap upon ligand entry. In PlmII-Pepstatin A complex, the distance between flaps reduced significantly to 9.9Å, indicating that the binding cavity closes to embrace the inhibitor (*6*). Thus, as evident from these measurements, the binding cavity of PlmII exhibits a rather flexible conformation which adapts to accommodate inhibitors based on their bulkiness.

However, the defined parameter as described by Asojo *et al.,* provide some information on the opening and closing motion of the flap-like structure, this single parameter was based on a rigid crystal structure and only described the motions in one-dimension ($\mathbf{d_1}$) of space (*6, 9*) (**Figure 1)**. Analysis of the MD trajectories clearly indicated that more parameters need to be defined to appropriately describe the flap motion (**see section 3.2**)

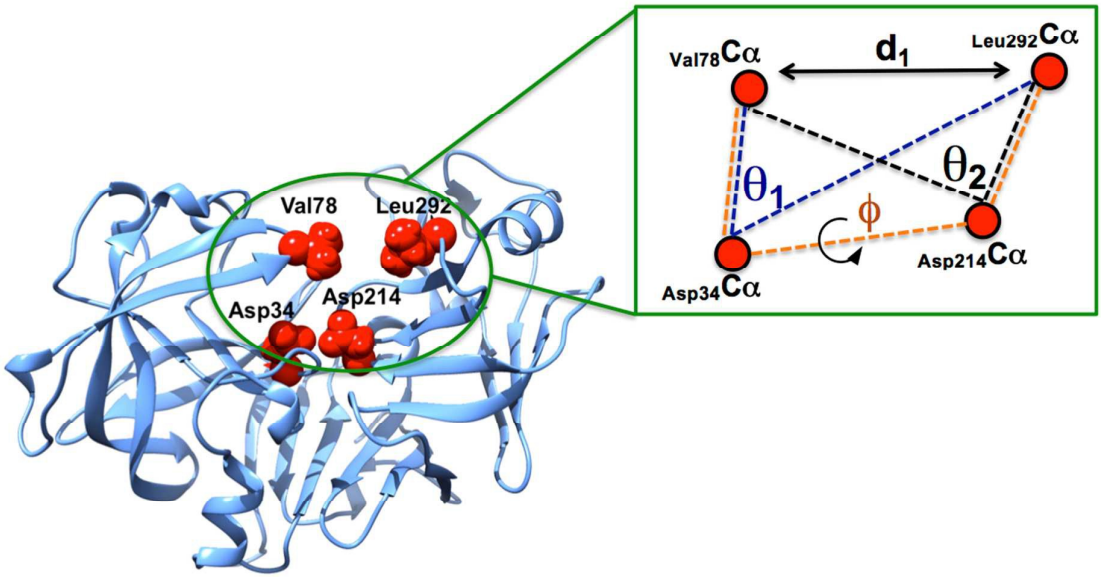

Figure 1. An illustration of the different proposed parameters to describe the flap motion; distance (d_1) between the flap tip residues (Val78, Leu292) and TriCα angles, θ_1, θ_2 and dihedral angle, ϕ

3.2. Proposed different parameters to describe flap opening and closing

Visual inspection of the molecular dynamic trajectory snapshots shows that the opening and closing of the binding cavity of the free PlmII structure is characterized by an extensive "twisting" of the flap and the concerted recoiling of a proline rich loop (flap-like structure).

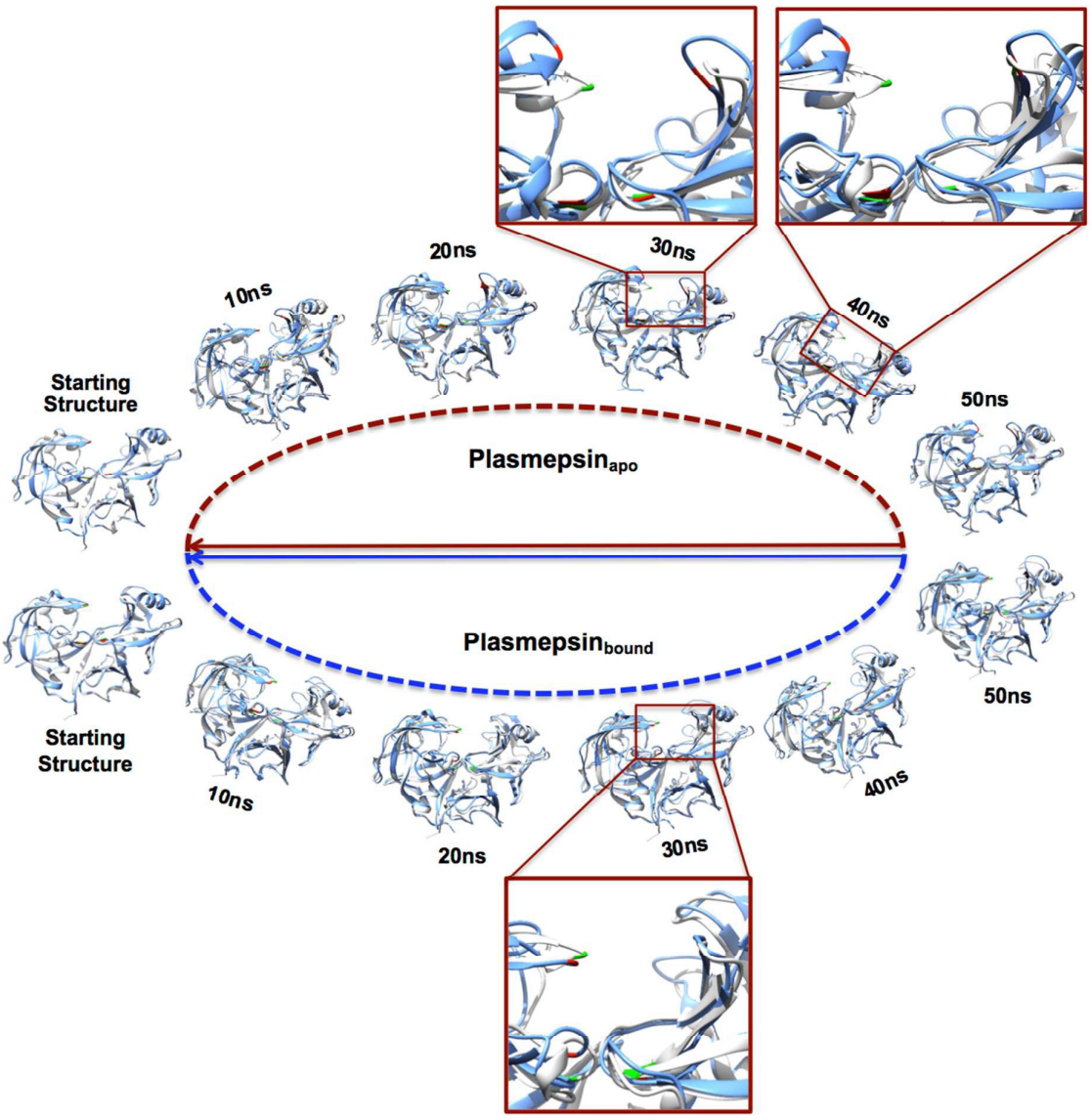

Figure 2. MD trajectory showing the flap dynamics of free and bound (PlmII-EH58) PlmII (blue ribbons) superimposed against the starting structure (grey ribbons). Flap tips for the free and bound are shown in green and red, respectively

Upon observation of the flap motions in PlmII (**Figure 2**), we propose that these motions can be explained accurately by considering the distance between flap tip residues ($\mathbf{d_1}$) in relation to the TriCα angles, Val78-Asp34-Leu292, $\boldsymbol{\theta_1}$ and Val78-Asp214-Leu292, $\boldsymbol{\theta_2}$ as well as the dihedral angle, $\boldsymbol{\phi}$ (**Figure 1).**

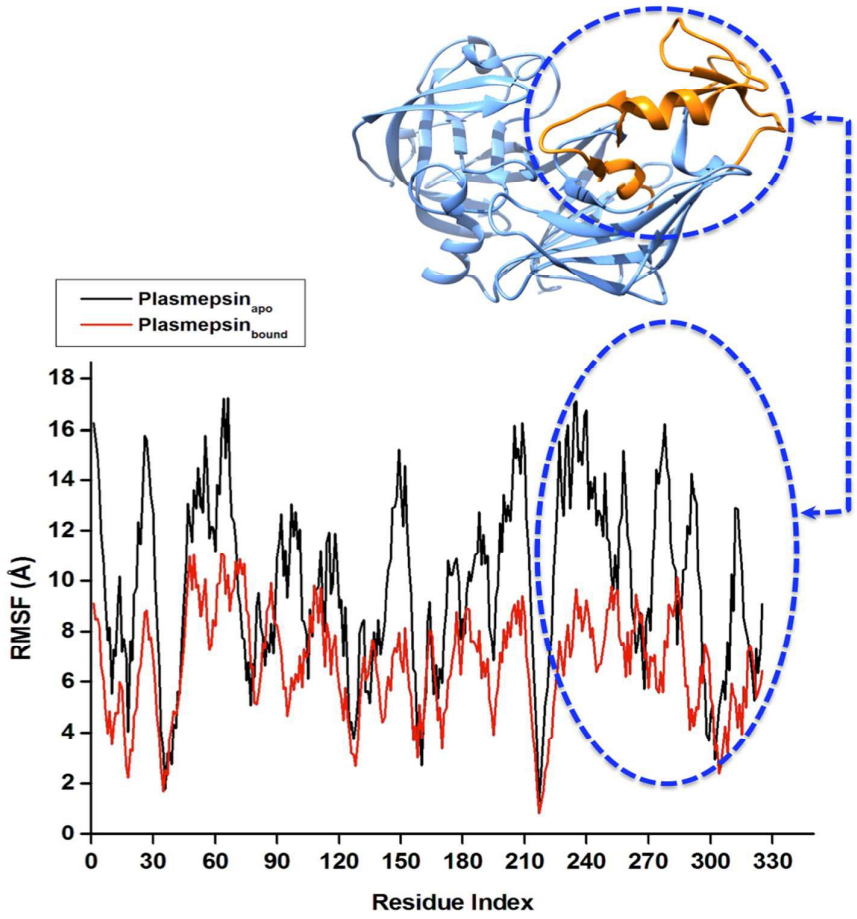

Figure 3. Plot of root mean square fluctuation (RMSF) of apo PlmII (blue) and PlmII-EH58 complex (red). Region showing high residual fluctuation corresponding to the proline-rich region of PlmII is shown in orange

The "twisting" of the flap and the lateral shift of the highly flexible loop in the open conformation appears to be a coordinated movement, involving the highly flexible loop a proline-rich region (223-295) (**Figure 3**). As evident from the root mean square fluctuation (RMSF) plot of the free and bound PlmII, the apo PlmII shows high residual fluctuation around this proline-region loop compared to the bound PlmII, indicating less residual interaction in the bound state of the enzyme. The average RMSF of the apo was 9.84Å, whereas it was 6.65Å for the bound enzyme, indicating a more compact bound enzyme with less residual fluctuations and a more flexible apo enzyme with high residual atomic fluctuations. Higher residual fluctuations were observed in the proline rich area, as well as the flap residues. The bound PlmII adopts a compact closed conformation all through the simulation, whereas in the free enzyme, the flexible regions adopt different conformations

with the opening and closing of the binding cavity. This loop, recoils inside the binding cavity towards the catalytic dyad (Asp34, Asp214) as it adopts a lateral shift away from the main enzyme structure. Interestingly, the residue at the tip (Leu292) of this loop moves relatively less compared to the entire loop. Notably, the intense motion at the highly flexible proline-rich loop seems not to orient Leu292 away from the binding cavity rather, the loop movement seems to cause steric hindrance on the flap tip residues resulting in the movement of the flap away from the binding cavity. The average radius of gyration (Rg) for the free PlmII was 7.88Å whereas for the bound it was ~2Å less; thus highlighting the rigorous asymmetrical opening and closing of the flap which may have led to changes in moment of inertia (**see supplementary information**).

As such, this intensive and coordinated flap motion may certainly not be defined by distance (d_1) alone, but rather a combination of parameters including TriCα angles (θ_1, θ_2) and dihedral angle, ϕ, as have been proposed in this paper. The distance, d_1, between flap tip residues was 10.67Å at the starting structure of the free enzyme. Partial flap opening was observed at ~30ns, with the full flap opening occurring at 46.8ns (d_1 = 23.61Å). Towards the end of the 50ns MD simulation, the closing of the flap was observed at 50ns (d_1 = 12.7Å). Further, for the first time we observed an asymmetrical opening of the binding cavity evident by the "twisting" of the flap and a maximum "twisting" at the time range of 22-31ns corresponding to a large shift in the dihedral angle, ϕ from -33.91° to +20.99°. Although "twisting" alone may not solely describe the extent of flap opening, it however reveals the asymmetrical nature of flap opening as defined by the dihedral angle, ϕ. This demonstrates the intensive motion which involves the movement of adjacent residues around the highly flexible loop which seems to generate steric hindrance that drives away the flap lying at the active site cavity.

3.3. **Defining the appropriate "Combined" Parameters**

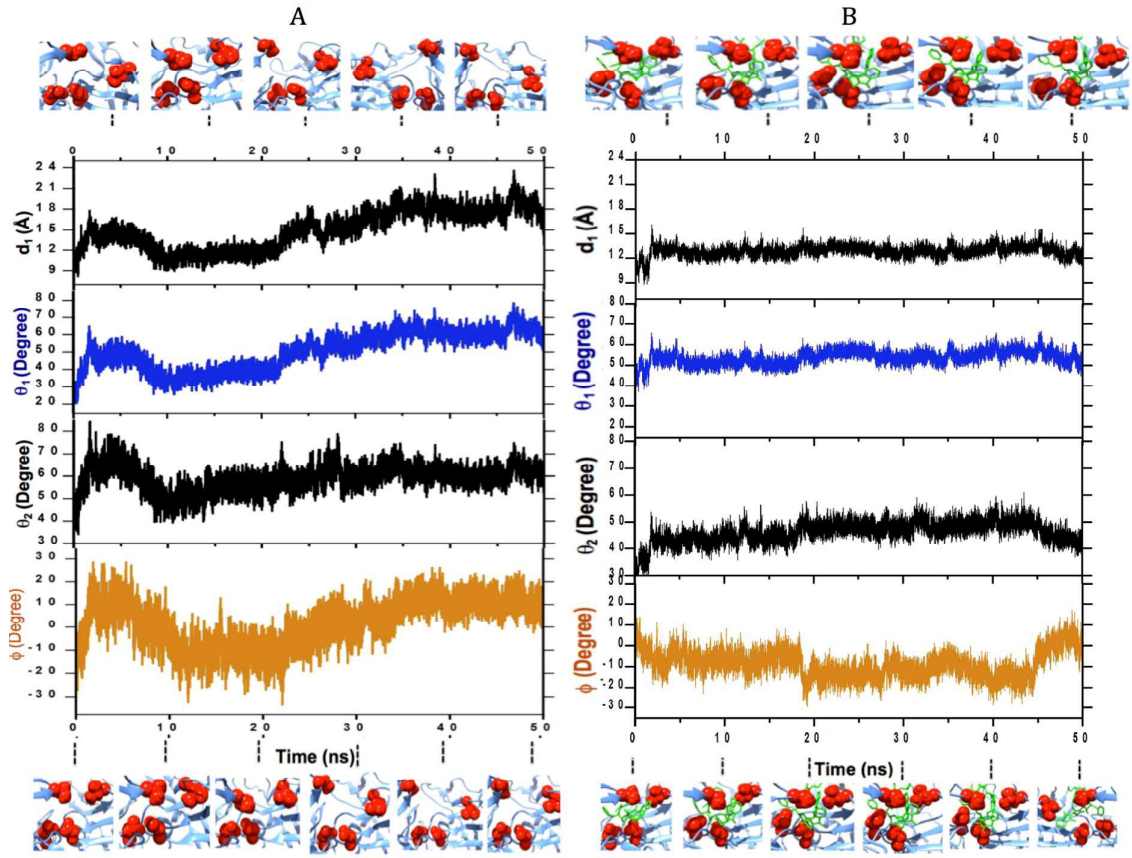

Figure 4. Combined plots of distance, d_1, between flap tip residues (Val78, Leu292), dihedral angle, ϕ, and TriCα angles, θ_1, θ_2 against time (ns) of the Apo PlmII [**A**] and PlmII-EH58 complex [**B**]

i. Distance, d_1, between flap tip residues and dihedral angle, phi (ϕ)

Plotting the dihedral angle, ϕ and distance, d_1 against time (ns) for the free PlmII (**Figure 4A**), it is evident that d_1 increases with an increase in the angle ϕ. A sharp increase in d_1 and ϕ corresponding to the partial opening of the active site cavity is observed at 30ns. This is consistent with the "twisting" motion of the flap as it moves away from the active site pocket. The partial opening of the active site cavity at 30ns is accompanied by an increase in the dihedral angle, ϕ which demonstrates that though movement is observed at the flaps, there is an intensive orientation of the peptide bond, evident by the large shift in the dihedral angle, ϕ, which results in a concerted movement of the flap away from the active site pocket.

In the PlmII-EH58 complex, there was no significant movement of the flap as the ligand (EH58) remained embraced by the flap at the active site cavity. The average distance between Val78 at the flap tip and Leu292 remained at 13Å across the 50ns simulation of the bound PlmII (**Figure 4B**).

ii. Distance, d_1 between flap tips and TriCα Angles, θ_1 and θ_2

Measuring the distance as well as the angle between the flap tip residues and the catalytic residues may better explain the flap dynamics in this protease. The aspartic residues sitting in the active site are observed to show minimal movement relative to the highly dynamic flap tip residues and the highly flexible loop. Interestingly, the trend in distance of Cα of Val78 and Leu292 highly correlates with the angle between Val78-Asp34-Leu292. However, the angle between Val78-Asp214-Leu292 did not accurately describe the flap movement observed in the MD simulation as well as the observed "twisting" of the flap structure to allow the opening of the binding cavity. Thus, the opening and closing of the binding cavity can better be explained by measuring the angle, θ_1, between Val78-Asp34-Leu292 and correlating it with the distance between Cα of the flap tip residues. The active site residue, Asp214, has a high atomic fluctuation compared to Asp34. This may be attributed to its closeness to the highly flexible proline-rich loop region located at the binding cavity rim. Thus, Asp214 is highly mobile and may not give an accurate representation of the "twisting" as well as the opening and closing of the flap.

In the PlmII-EH58 complex, there was no observed drastic fluctuation in the TriCα angles, θ_1 and θ_2. Average angle during the 50ns simulation was ~46°. This trend is similar to the observed minimal changes in the d_1 during the 50ns simulation average distance between Val78 at the flap tip and Leu292 remained at 13Å across the 50ns simulation of the bound PlmII (**Figure 4B**).

This study will ultimately contribute to the design of potent structure-based inhibitors against plasmepsins such as allosteric inhibitors targeting flap pockets, thus inhibiting the opening and closing of the binding cavity. Further, the parameters proposed in this study may be extended in determining flap opening and closing in other aspartic proteases involved in disease.

4. Conclusion

The binding cavity of plasmepsin has been observed to adapt to different inhibitors demonstrating its plasticity. Precise parameters to define flap motion in plasmepsin will certainly assist in the design of potent inhibitors to bind to the flexible binding cavity. In addition, recent identification of flap pockets for potent non-peptidomimetic inhibitors further raises the important of this study.

In conclusion, the asymmetrical flap opening and closing was evident, characterized by a "twisting" motion. Only three parameters we postulated namely distance, dihedral angle and TriCα angles which appropriately defined the observed "twisting' motion during the flap opening and closing. However, the extensive motion of a proline-rich loop adjacent to the binding cavity rim appeared to exert steric hindrances on the flap residues, driving the flap away from the active site cavity. This loop may also have increased movements around the catalytic dyad residue, Asp214, resulting in the observed distortion of the TriCα angle, θ_2. Overall the average θ_1 and θ_2 for the bound was ~46° and ~53°, respectively compared to ~50° and ~59° for the Apo PlmII, indicating intensive changes in the TriCα as the active site cavity opens. Similar trends in the distance, d_1 and dihedral angle, ϕ were observed during the simulation. The asymmetrical opening of the binding cavity was best described by the large shift of -33.91° to +20.99° in the ϕ, corresponding to the partial opening of the flap at a range of 22-31ns. Though, the dihedral angle describes the twisting of the flap, the extent of flap opening can be defined by combining the distance,d_1 and the Val78-Asp34-Leu292 TriCα angle, θ_1. The results presented here on the combined parameters will certainly augment current efforts in designing potent structure-based inhibitors against plasmepsins.

5. Acknowledgement

The authors like to acknowledge the School of Health Sciences, University of KwaZulu-Natal, and Westville for financial support.

6. Conflicts of Interests

Authors declare no conflicts of interest.

References

1. Gil L, A., Valiente, P. A., Pascutti, P. G., and Pons, T. (2011) Computational perspectives into plasmepsins structure-function relationship: implications to inhibitors design, *Journal of tropical medicine 2011*, 657483-657483.
2. Greenwood, B., Bojang, K., Whitty, CJ., Targett, GA. . (2005) Malaria, *Lancet 365*, 1487-1498.
3. Greenwood, B. (2014) Treatment of Malaria - A Continuing Challenge, *New England Journal of Medicine 371*, 474-475.
4. Bhaumik, P., Gustchina, A., and Wlodawer, A. (2012) Structural studies of vacuolar plasmepsins, *BBA-Proteins Proteomics 1824*, 207-223.
5. Banerjee, R., Liu, J., Beatty, W., Pelosof, L., Klemba, M., and Goldberg, D. E. (2002) Four plasmepsins are active in the Plasmodium falciparum food vacuole, including a protease with an active-site histidine, *Proceedings of the National Academy of Sciences of the United States of America 99*, 990-995.

6. Asojo, O. A., Gulnik, S. V., Afonina, E., Yu, B., Ellman, J. A., Haque, T. S., and Silva, A. M. (2003) Novel uncomplexed and complexed structures of plasmepsin II, an aspartic protease from Plasmodium falciparum, *Journal of Molecular Biology 327*, 173-181.
7. Bhaumik, P., Horimoto, Y., Xiao, H., Miura, T., Hidaka, K., Kiso, Y., Wlodawer, A., Yada, R. Y., and Gustchina, A. (2011) Crystal structures of the free and inhibited forms of plasmepsin I (PMI) from Plasmodium falciparum, *Journal of Structural Biology 175*, 73-84.
8. Bhaumik, P., Xiao, H., Parr, C. L., Kiso, Y., Gustchina, A., Yada, R. Y., and Wlodawer, A. (2009) Crystal Structures of the Histo-Aspartic Protease (HAP) from Plasmodium falciparum, *Journal of Molecular Biology 388*, 520-540.
9. Asojo, O. A., Afonina, E., Gulnik, S. V., Yu, B., Erickson, J. W., Randad, R., Medjahed, D., and Silva, A. M. (2002) Structures of Ser205 mutant plasmepsin II from Plasmodium falciparum at 1.8 angstrom in complex with the inhibitors rs367 and rs370, *Acta Crystallographica Section D-Biological Crystallography 58*, 2001-2008.
10. Ishima, R., and Louis, J. M. (2008) A diverse view of protein dynamics from NMR studies of HIV-1 protease flaps, *Proteins-Structure Function and Bioinformatics 70*, 1408-1415.
11. Cai, Y., Yilmaz, N. K., Myint, W., Ishima, R., and Schiffer, C. A. (2012) Differential Flap Dynamics in Wild-Type and a Drug Resistant Variant of HIV-1 Protease Revealed by Molecular Dynamics and NMR Relaxation, *Journal of Chemical Theory and Computation 8*, 3452-3462.
12. Hornak, V., Okur, A., Rizzo, R. C., and Simmerling, C. (2006) HIV-1 protease flaps spontaneously open and reclose in molecular dynamics simulations, *Proceedings of the National Academy of Sciences of the United States of America 103*, 915-920.
13. Scott, W. R. P., and Schiffer, C. A. (2000) Curling of flap tips in HIV-1 protease as a mechanism for substrate entry and tolerance of drug resistance, *Structure 8*, 1259-1265.
14. Ishima, R., Freedberg, D. I., Wang, Y. X., Louis, J. M., and Torchia, D. A. (1999) Flap opening and dimer-interface flexibility in the free and inhibitor-bound HIV protease, and their implications for function, *Structure with Folding & Design 7*, 1047-1055.
15. Toth, G., and Borics, A. (2006) Flap opening mechanism of HIV-1 protease, *Journal of Molecular Graphics & Modelling 24*, 465-474.
16. Galiano, L., Bonora, M., and Fanucci, G. E. (2007) Interflap distances in HIV-1 protease determined by pulsed EPR measurements, *Journal of the American Chemical Society 129*, 11004-+.
17. Hornak, V., Okur, A., Rizzo, R. C., and Simmerling, C. (2006) HIV-1 protease flaps spontaneously close to the correct structure in simulations following manual placement of an inhibitor into the open state, *Journal of the American Chemical Society 128*, 2812-2813.
18. Galiano, L., Ding, F., Veloro, A. M., Blackburn, M. E., Simmerling, C., and Fanucci, G. E. (2009) Drug Pressure Selected Mutations in HIV-1 Protease Alter Flap Conformations, *Journal of the American Chemical Society 131*, 430-+.
19. Heaslet, H., Rosenfeld, R., Giffin, M., Lin, Y.-C., Tam, K., Torbett, B. E., Elder, J. H., McRee, D. E., and Stout, C. D. (2007) Conformational flexibility in the flap domains of ligand-free HIV protease, *Acta Crystallographica Section D-Biological Crystallography 63*, 866-875.

20. Kovalskyy, D., Dubyna, V., Mark, A. E., and Kornelyuk, A. (2005) A molecular dynamics study of the structural stability of HIV-1 protease under physiological conditions: The role of Na+ ions in stabilizing the active site, *Proteins-Structure Function and Bioinformatics 58*, 450-458.
21. Prade, L., Jones, A. F., Boss, C., Bildstein, S. R., Meyer, S., Binkert, C., and Bur, D. (2005) X-ray structure of plasmepsin II complexed with a potent achiral inhibitor, *Journal of Biological Chemistry 280*, 23837-23843.
22. Zuercher, M., Gottschalk, T., Meyer, S., Bur, D., and Diederich, F. (2008) Exploring the flap pocket of the antimalarial target plasmepsin II: The "55% rule" applied to enzymes, *Chemmedchem 3*, 237-240.
23. H.M. Berman, J. W., Z. Feng, G. Gilliland, T.N. Bhat, H. Weissig, I.N. Shindyalov, P.E. Bourne (2000) The Protein Data Bank, *Nucleic Acids Research 28.*, 235-242.
24. Karubiu, W., Bhakat, S., and Soliman, M. E. S. (2014) Compensatory Role of Double Mutation N348I/M184V on Nevirapine Binding Landscape: Insight from Molecular Dynamics Simulation, *The protein journal 33*, 432-446.
25. Bhakat, S., Martin, A. J. M., and Soliman, M. E. S. (2014) An integrated molecular dynamics, principal component analysis and residue interaction network approach reveals the impact of M184V mutation on HIV reverse transcriptase resistance to lamivudine, *Molecular BioSystems 10*, 2215-2228.
26. D.A. Case, V. B., J.T. Berryman, R.M. Betz, Q. Cai, D.S. Cerutti, T.E. Cheatham, III, T.A. Darden, R.E. Duke, H. Gohlke, A.W. Goetz, S. Gusarov, N. Homeyer, P. Janowski, J. Kaus, I. Kolossváry, A. Kovalenko, T.S. Lee, S. LeGrand, T. Luchko, R. Luo, B. Madej, K.M. Merz, F. Paesani, D.R. Roe, A. Roitberg, C. Sagui, R. Salomon-Ferrer, G. Seabra, C.L. Simmerling, W. Smith, J. Swails, R.C. Walker, J. Wang, R.M. Wolf, X. Wu and P.A. Kollman. (2014) AMBER 14, University of California, San Francisco.
27. Bhakat, S., Martin, A. J. M., and Soliman, M. E. S. (2014) An Integrated Molecular Dynamics, Principal Component Analysis and Residue Interaction Network Approach Reveals the Impact of M184V Mutation on HIV Reverse Transcriptase Resistance to Lamivudine, *Molecular BioSystems*.
28. Pettersen, E. F., Goddard, T. D., Huang, C. C., Couch, G. S., Greenblatt, D. M., Meng, E. C., and Ferrin, T. E. (2004) UCSF chimera - A visualization system for exploratory research and analysis, *Journal of Computational Chemistry 25*, 1605-1612.